Proceedings of the
Annual Stability Conference
Structural Stability Research Council
San Antonio, Texas, March 21-24, 2017

The Effects of Accurate Boundary Condition Modeling on Column Stability

Cliff D. Bishop[1] and Patxi Uriz[2]

Abstract
Idealization of real-world boundary conditions as either "free," "pinned," or "fixed" is common in engineering practice. Standard generalization of end restraints can lead to conservative designs. However, certain instances may merit the additional calculation effort for a more realistic boundary condition for a higher degree of accuracy. Some examples include: the optimization of hundreds of similar connections, verification of as-built details, or a detailed understanding of the moment transfer at the base of a structure. This paper explores the effect on column stability of an example connection through rigorous finite element analysis and nonlinear, load-deflection models. Abaqus is used to assess the moment-rotation capacity of a suite of connections representing commonly encountered boundary conditions. Parameters such as variable axial loads, contact or bearing within the connection, and component yielding are incorporated into the FEA model. The results of the FEA are used in OpenSees to determine the column capacity through a large-displacement, inelastic analysis. Finally, a comparison of the column capacity is made between the in-situ and ideal connection models to provide engineering insight into the importance of accurately modeling connections.

1. Background

Engineers often encounter in-situ support conditions that differ from the theoretical conditions that are taught at university. These conditions may prove difficult to assess how much freedom (or lack thereof) of movement is actually allowed between the member and the base or surrounding structure. If highly-accurate prediction of buckling capacity or determination of forces/stresses is important, then any uncertainty in the amount of restraint provided by the support conditions can unduly influence the calculations.

Classical formulations and solutions to differential equations governing column/beam stability are found in many texts including, e.g., Timoshenko and Gere (1961) and Chen and Liu (1987). The simplest problems involve columns with theoretically "pinned" or "fixed" boundary conditions subject to concentric axial load. More advanced solution techniques are required to address the effects of elastic restraint or other loading conditions. Whether solutions are based on bifurcation instabilities or load-deflection solutions, the proper consideration of boundary conditions can play a pivotal role in ensuring an accurate critical load prediction.

[1] Ph.D., P.E., S.E., Senior Engineer, Exponent, Inc., cbishop@exponent.com
[2] Ph.D., P.E., Principal Modeler, Risk Management Solutions, Patxi.Uriz@RMS.com

2. Idealized Boundary Conditions

2.1 Basic Conditions

Most texts on structural analysis provide characteristics of various idealized support conditions. Some examples of typical idealized boundary conditions are shown in Figure 1 (Leet and Uang, 2005). A summary of six main types of supports and their prevented or allowed translations and rotations is provided in Table 1.

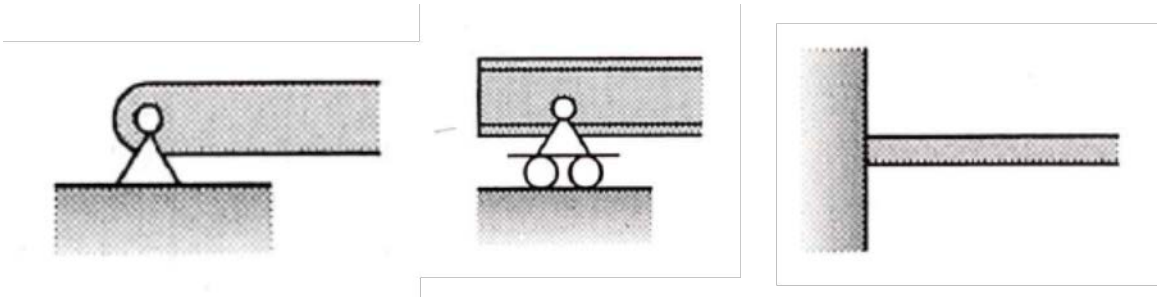

(a) (b) (c)

Figure 1: Typical Supports – pinned (a), roller (b), fixed (c) (Leet and Uang, 2005)

Table 1: Summary of Supports

Type	Prevented	Allowed
Roller	Δ_y	Δ_x, θ
Link[1]	Δ	Δ, θ
Guide	Δ_y, θ	Δ_x
Pin	Δ_x, Δ_y	θ
Hinge[2]	Δ	Δ, θ
Fixed	Δ_x, Δ_y, θ	-

[1] No translation in axial direction of link; translation perpindicular to link allowed.

[2] No relative translation of member ends at joint; translation and rotation of joint allowed.

For conditions when the in-situ supports match one of these idealized supports, the "prevented" translations (Δ) and rotations (θ) shown in Table 1 can be used to remove unknowns in the systems of differential equations and to determine the predicted load at incipient buckling. It should be noted that the idealized joints described in this section are assumed to be friction free. The question then becomes: How does one determine the stability of systems with supports that differ from the idealized conditions?

2.2 Classical Solutions to Elastic Restraints

The classical equations for determining the end moments for a beam with both ends fixed and a transverse point load are shown in Eq. 1 (Timoshenko and Gere, 1961):

$$\theta_a = 0 = \theta_{0_a} + \frac{M_a l}{3EI}\psi(u) + \frac{M_b l}{6EI}\phi(u)$$
$$\theta_b = 0 = \theta_{0_b} + \frac{M_a l}{6EI}\phi(u) + \frac{M_b l}{3EI}\psi(u) \quad (1)$$

where θ_a and θ_b are the rotation at each of the ends, M_a and M_b are the moments at each of the ends, θ_{0a} and θ_{0b} are the angles of rotation of the beam ends assuming the ends are hinged, $\psi(u)$ and $\phi(u)$ are trigonometric factors representing the influence of the axial force on the beam end rotation angles, and l is the beam length.

For the case where the ends are *not* fixed, Eq. 1 must be revised to consider the degree of rotation allowed at each end of the beam. The moments at each end can be expressed as in Eq. 2 (Timoshenko and Gere, 1961):

$$M_a = -\alpha\theta_a \quad M_b = -\beta\theta_b \quad (2)$$

where α and β are coefficients that define the degree of end restraint supplied by the partial-fixity boundary condition and the other variables have been defined previously. The restraint coefficients can vary from zero for the case of pinned ends to infinity for fixed ends. Substituting Eq. 2 into Eq. 1 (and removing the condition that θ_a and θ_b equal zero) results in Eq. 3 (Timoshenko and Gere, 1961):

$$\theta_a = \frac{-M_a}{\alpha} = \theta_{0_a} + \frac{M_a l}{3EI}\psi(u) + \frac{M_b l}{6EI}\phi(u)$$
$$\theta_b = \frac{-M_b}{\beta} = \theta_{0_b} + \frac{M_a l}{6EI}\phi(u) + \frac{M_b l}{3EI}\psi(u) \quad (3)$$

where all terms are defined previously. Eq. 3 can be solved for the end moments once α and β have been determined.

2.3 AISC Alignment Chart

The American Institute of Steel Construction (AISC) provides one method for determining the fixity at each end of a column in the Commentary to the Specification §7.2 (AISC 360-10). When the column is fixed at both ends, the theoretical effective length factor, *K*, is equal to 0.5. Conversely, when the column is pinned at each end, *K* = 1.0. Plugging these values for *K* into the Euler buckling equation yields a critical load four-times greater for the case of the fixed-ended vs pinned-ended conditions.

For the case where the end restraints are somewhere in between pinned and fixed, use of the AISC alignment charts is applicable. The alignment charts for either sidesway inhibited (e.g., braced frames) or sidesway uninhibited (e.g., moment frames) can be referenced after first determining the relative stiffness of the columns and girders framing into each joint at the ends of the column in question. When the columns are significantly stiffer than the beams framing into the joint, little restraint is provided to keep the column end from rotating, thus approaching the condition of a

pinned support. Conversely, when the beams are significantly stiffer than the columns framing into the joint, significant restraint may be provided, effectively fixing the base of the subject column. Once the relationship between the column and beam stiffness is known, an appropriate value of *K* can be selected from the charts. For the case of braced frames, *K* practically varies between the values of 0.5 and 1.0 as discussed above.

3. Realistic Boundary Conditions

In contrast to the preceding section's discussion of theoretical boundary conditions, the focus herein lies with as-built, realistic boundary conditions. Figure 2 and Figure 3 show boundary conditions that have been observed in the field. While it may be possible (and even practical) to idealize these conditions for use in computer models or hand calculations, the support simplification may alter (potentially significantly) the predicted buckling load of the structural member in question and transfer unexpected forces to other elements/members.

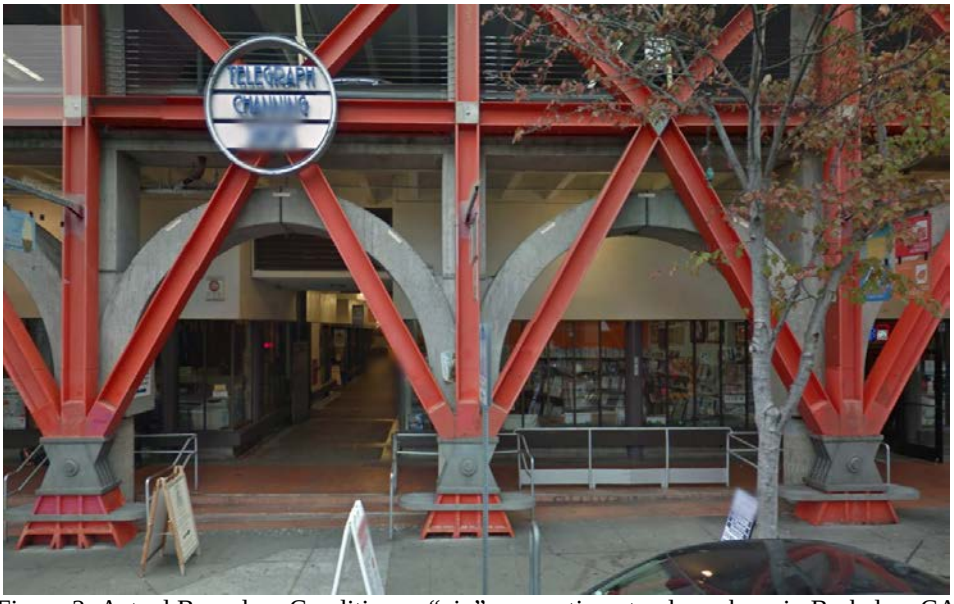

Figure 2: Actual Boundary Conditions - "pin" connection at column base in Berkeley, CA (source: maps.Google.com)

Figure 3: Actual Boundary Conditions –gusset plate for bracing members at the Ferry Building in Oakland, CA

3.1 Moment-rotation Curves

Between the two extremes of a fully-pinned condition and a fully-fixed condition lies a continuum of conditions where partial fixity influences the response. If the response of the connection can be represented by a rotational spring (elastic or inelastic), then a common method for visualizing the connection capacity is through a moment-rotation curve. This type of plot graphically depicts Eq. 2 for various restraint coefficients. Examples of moment rotation curves are shown in Figure 4 (Steel 1992).

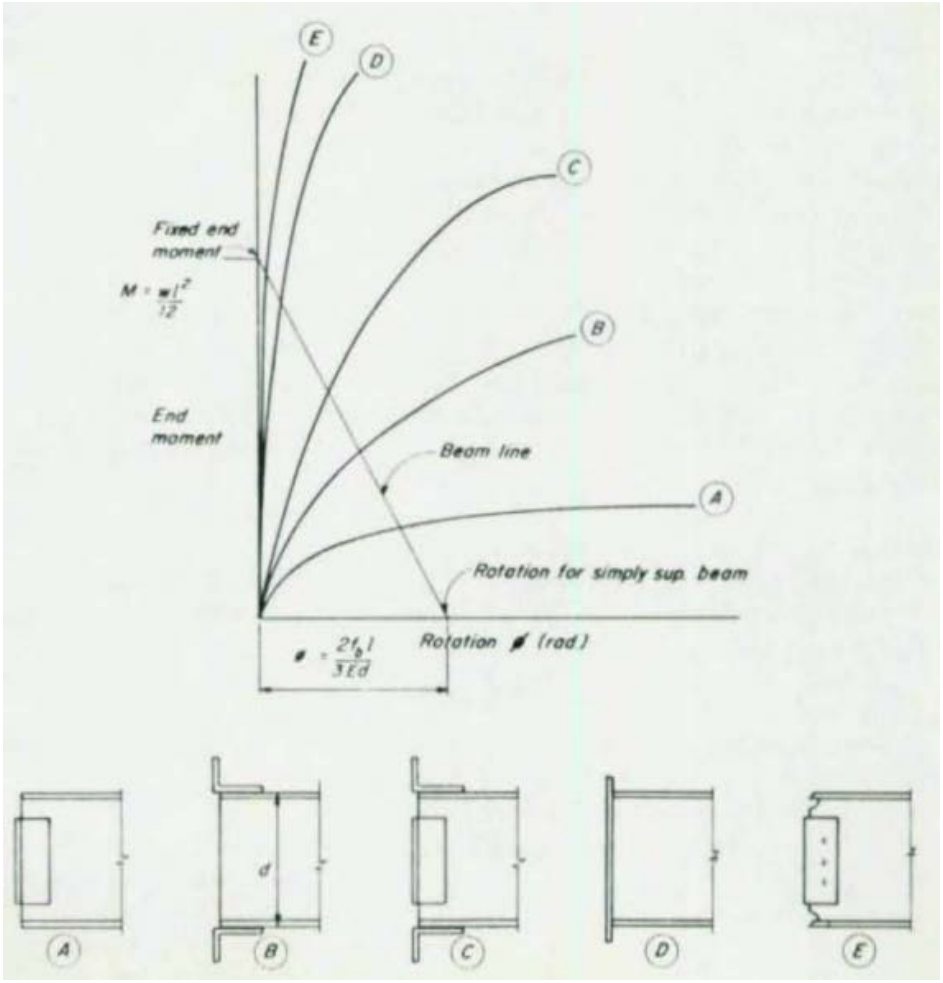

Figure 4: Sample Moment-Rotation Plots (source: Steel 1992)

After the relationship between moment and rotation has been established for the in-situ support, a curve similar to one shown in Figure 4 can be used to solve Eq. 3 or implemented into a computer-aided structural analysis. The most common method of implementing the partial restraint in a computer model is through the use of a rotational spring.

3.2 Example Description

The example presented involves boundary condition modeling for a simple, two-story steel braced frame as shown in Figure 5. Bracing is provided out-of-plane only at the beam-column joints at both levels. The base of the frame is arbitrarily depicted in the figure and will be discussed in detail

later. All of the beams and braces have friction-free hinges at each end. The span of the frame is twenty-five feet. The first story is twenty-one feet and the second story is twelve feet.

All top and bottom beams are rolled, wide-flange sections W14x211. The columns are W14x283. The braces are round, hollow structural steel (HSS) tube sections HSS10.75x0.5.

The frame is loaded with two loads, each of equivalent magnitude and placed concentrically at the top of each column. Initial imperfections are applied to the column members based on construction tolerances stipulated in the Code of Standard Practice (AISC 303-10). The imperfections are applied at the intersection of the beams and braces and are selected to cause the most deleterious effects on the bracing system. The magnitude of the out-of-plane imperfection is roughly 1/800 of the total length of the member.

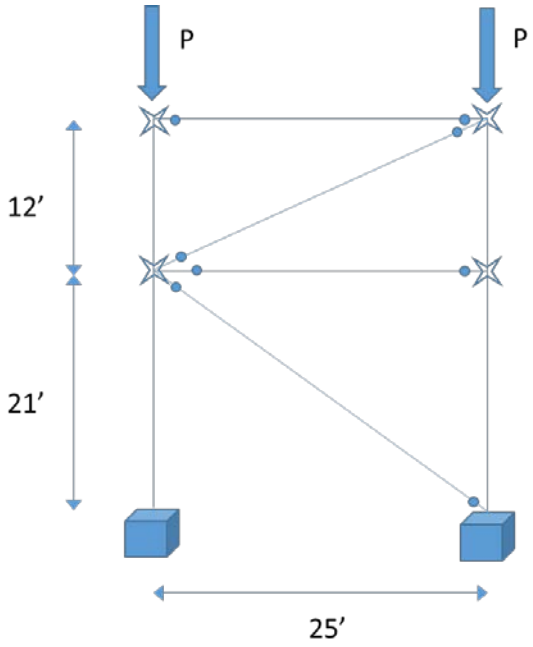

Figure 5: Example Braced Frame

The support condition at the base of the frame columns is a pin-in-a-cup. The pin has either a flat-bottom surface or a radiused surface (the radiused case is rendered in Figure 6). The as-built pin (and connected column) rotates in the cup, creating contact between the face of the pin and the inside of the cup. The pin deflection is restrained by contact and deformation of the cup, thereby adding rotational stiffness to the boundary condition. The point of this example is to load the frame to failure by incrementally increasing the applied load *P* while varying the level of restraint provided at the column base. The large axial load, contact, and subsequent cup deformation provides some stiffness, thus the true restraint lies somewhere between the theoretical pinned or fixed conditions.

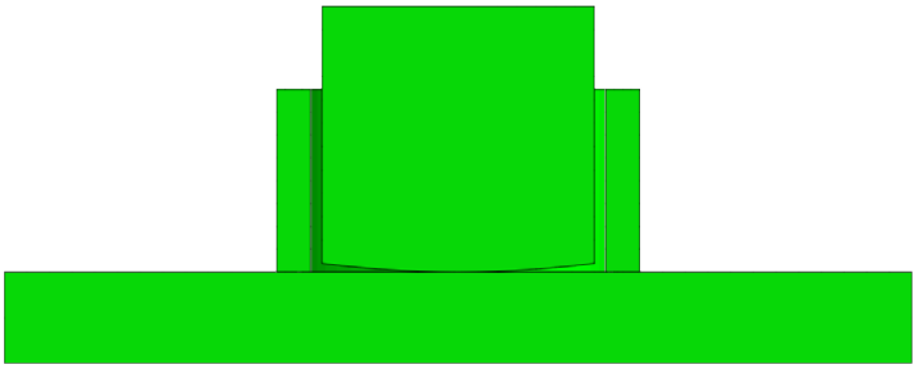

Figure 6: Radiused pin-in-cup cross section

3.3 Modeling Techniques

The frame is initially modeled in OpenSees based on the geometry depicted in Figure 5 and sections and materials discussed previously (2013). As a true "pin" connection does not permit translation yet freely permits rotation, a simplified pinned connection in OpenSees is predicted to provide a lower-bound solution to the true capacity of the frame. An additional analysis is performed in OpenSees using "fixed-ended" boundary conditions in order to provide an upper-bound for the true solution.

With the first two analyses performed based on the bounding theoretical support conditions, a third analysis is performed based on a refinement of the boundary conditions. A separate model is targeted to assess the rotational stiffness provided by pin-in-a-cup model. Along with the effect of the contact, the amount of axial loading in the column and the effect of yielding were considered to be deserving of scrutiny in the refined models.

In order to address the aforementioned refinement, Abaqus is employed to complement the effort in OpenSees (2011). Specifically, Abaqus is used to capture the more realistic mechanics of the boundary conditions shown in Figure 6. Once the refined model captures the true relationship between moment and rotation for the in-situ condition, the results are then imported into OpenSees and assigned to a spring at the base of the columns. The following sections detail some of the more important considerations when considering the base condition.

3.3.1 Software and Settings

OpenSees, (version 2.5.0) is used to model the structural system (2013). Primarily intended for earthquake engineering simulation, the Open System for Earthquake Engineering Simulation is an object oriented, open source structural software framework. OpenSees is research-grade software with significant contributions from researchers around the world. The structural framework allows users to expand the extensive element and material libraries. Instabilities are modeled via large-displacement local-to-global force transformation based on a co-rotational formulation, provided by Souza (2000). Each beam and column element is discretized into two displacement-based elements with five integration points each. Each integration point consists of a fiber cross section comprised of Giuffre-Menegotto-Pinto steel uniaxial material with F_y of 55ksi.

Abaqus, version 6.11-1 is used to model and perform the refined finite element analysis of the support condition (2011). All components are modeled with 3D solid finite elements. A static, general analysis procedure with two steps (both including nonlinear geometry) is used. Step 1 is the application of the prescribed axial load, which varies as described below. Step 2 involves incrementing the rotation of the pin. After the analysis is complete, a plot of moment versus rotation is created and the data is used to create the rotational spring for the OpenSees models.

3.3.2 Material Nonlinearity

The pin and cup are constructed from A572-Gr.55 steel with a nominal yield stress of 55 ksi. The cup is assumed to have an ultimate tensile stress equal to 70 ksi and the effects of strain hardening are included in the model. Spread of plasticity is tracked in the cup throughout the analysis. The pin and the base plate are assumed to remain elastic.

3.3.3 Pin Location and Contact

At some point, as the pin rotates in the cup, the pin interacts with the lip of the cup. The cup initially provides elastic restraint to the pin's movement. As the pin continues to rotate and the cup begins to deform significantly, the cup begins to yield and eventually will fully plastify. At this point, further rotation of the pin is met with little increase in resistance but a significant increase in deformations. This effect is captured in Abaqus through an interaction between the pin and the cup or base plate known as "contact." The contact permits one element to react or pull away from another. Friction is also considered between the pin and the cup and the pin and the base plate with a factor equal to 0.5.

3.3.4 Axial Loading

The performance of the pin-cup support assembly is dependent on the magnitude of the axial load applied to the column. Figure 7 shows the free-body diagram of the pin-cup assembly. The prescribed axial load is applied in Step 1, leading to a uniform force distribution at the interface between the bottom of the pin and the top of the base plate. Step 2 is the application of a displacement at the top of the pin, causing a rotation, in this case, about the bottom right corner of the pin. As the pin rotates, the force distribution at the pin-to-base plate interface changes resulting in varying restraint properties for different magnitudes of applied axial load.

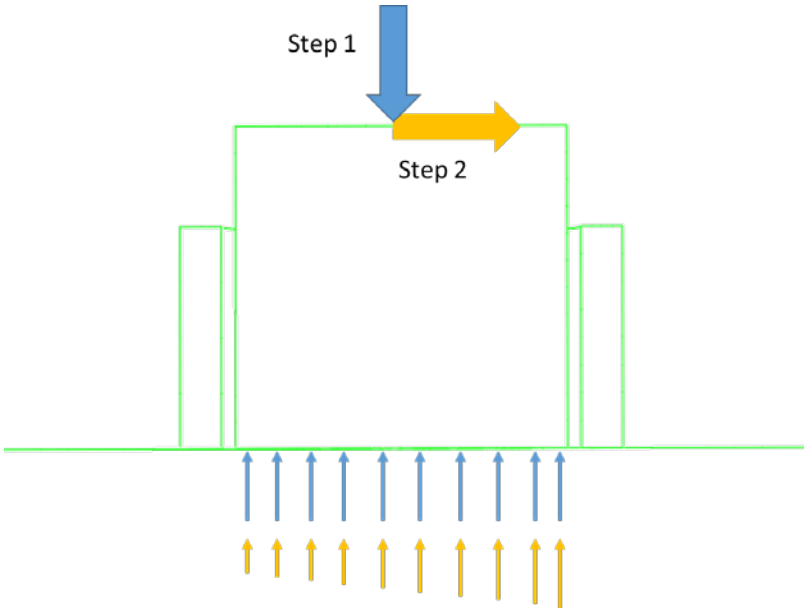

Figure 7: Free-Body Diagram

4. Results

4.1 Flat Pin

The first suite of results corresponds to modeling of the bottom surface of the pin as flat. That is, the pin is assumed to be initially in contact with the base plate along its entire surface. A cross-section rendering of this condition is shown in Figure 8.

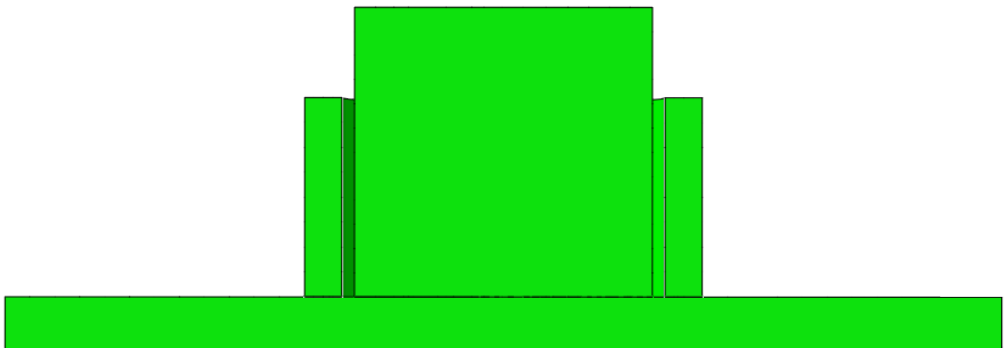
Figure 8: Flat pin-in-cup cross-section

4.1.1 Effect of Pin Location

The diameter of the cup and the pin differ such that a gap exists around the pin when centered in the cup (see, e.g., Figure 8). Since the bearing (contact) of the pin on the cup lip provides restraint (as discussed previously), the initial position of the pin and when it contacts the cup is of significance. Three models are created to address this case, all assuming movement of the top of the pin to the right as shown in Figure 8: 1) the pin centered in the cup, 2) the pin abutting the near side of the cup in the direction toward which the top of the pin is moving, and 3) the pin abutting the far side of the cup, opposite the direction toward which the top of the pin is moving. The results of these three analyses are shown in Figure 9 with an applied axial load of 400 kips.

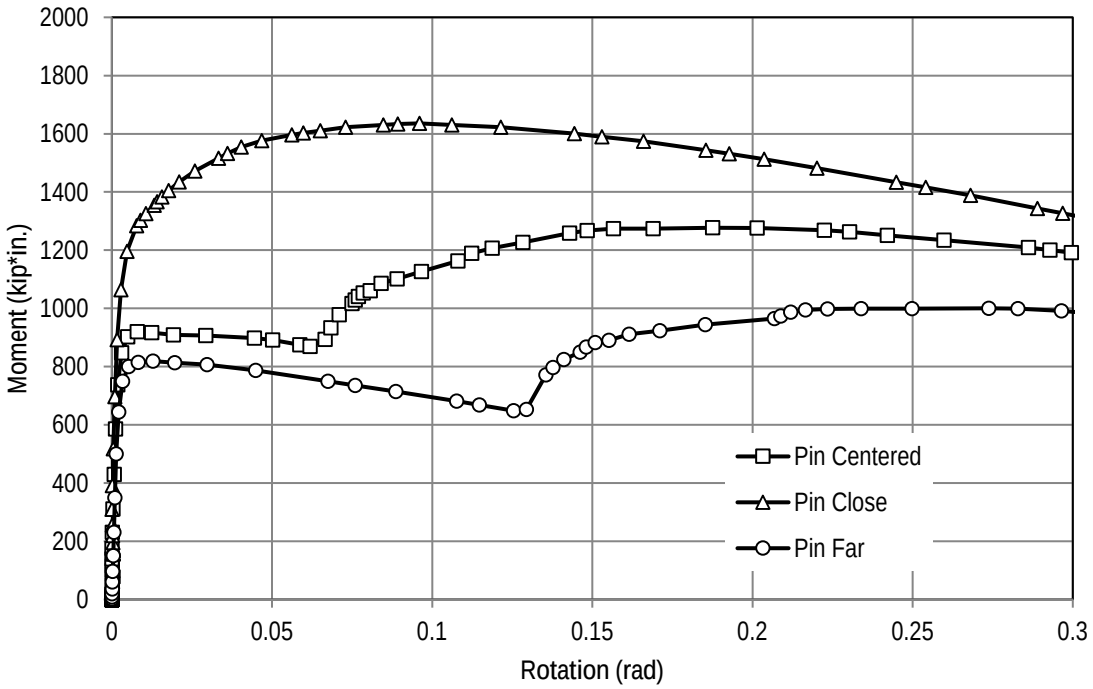

Figure 9: Variable Pin Location with Axial Load = 400 kips

For the case of the centered pin, there are three distinct regions of the plot:

1) Up to approximately 0.005 radians, the plot is fairly linear. The moment capacity is provided by the high axial load transmitted by the pin, i.e., the rotational restraint provided is mostly due to the pin's own ability to resist overturning.
2) From 0.005 radians up to 0.06 radians, the pin base that is in the direction of the applied rotation is still bearing on the base plate, but the far end of the pin has started to lift off the base plate. Contact may have occurred between the pin and the cup.
3) From 0.065 radians onward, the pin is in contact with the cup. The contact causes deformation and yielding of the cup. The highly non-linear nature of this region of the plot is consistent with the spread of plasticity within the cup material.

In contrast to the curve for the centered pin, the pin that is directly abutting the face in the direction in which the pin is moving ("pin close"), contact with the cup occurs almost immediately after the pin begins to tip toward the cup (around 0.005 radians). The cup then begins to deform and yield as before, and increases the magnitude of the force prior to yielding/uplift of the pin.

When the pin is abutting the face of the cup opposite the direction of movement ("pin far"), the initial stiffness still comes from bearing of the pin on the base plate. The pin continues to rotate and lift off the base plate. For the rotations plotted in Figure 9, the pin does not contact the cup until 0.13 radians.

4.1.2 Effect of Axial Load

The effect of increasing the axial load on the pin-cup support assembly is shown in Figure 10. These curves are created for the case when the pin is centered in the cup. Three levels of axial load are applied: 300, 400, and 500 kips. As the axial load increases, the curves shift toward higher

moment capacity for the same relative rotations. The most important aspect presented by these curves is the effect of the pin for self-restraint, i.e., up to 0.005 radians. For greater magnitudes of axial load, the pin's ability to restrain itself against overturning provides the basis for the increase moment capacity (and stiffness) of the connection.

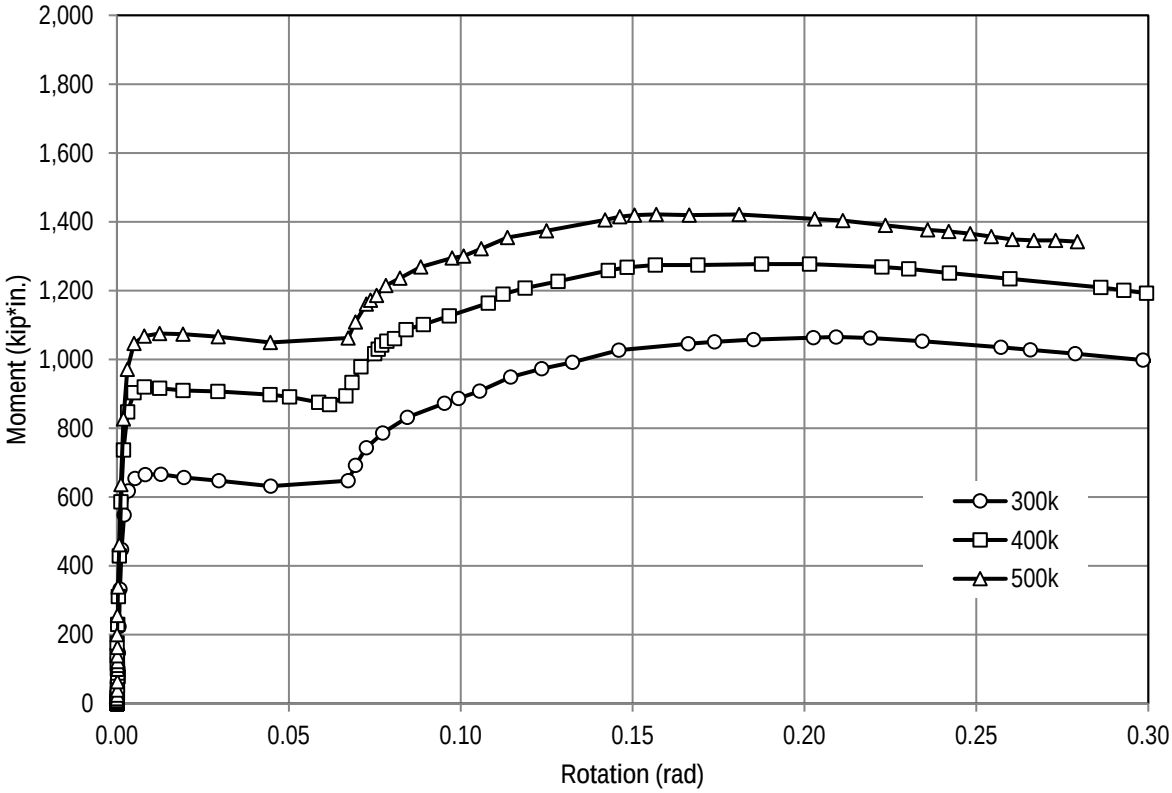

Figure 10: Effect of Axial Load for Centered Flat-bottom Pin

4.2 Radiused Pin

The second suite of results corresponds to modeling of the bottom surface of the pin as radiused. That is, the pin is assumed to be initially curved and is only in contact with the base plate over a limited region. A cross-section rendering of this condition was shown previously in Figure 6. The radiused pin condition was selected to ascertain the effects of the pin's ability to resist overturning in comparison to the case with the flat-bottom pin. A plot of the curves for various axial loading of the radiused pin is shown Figure 11.

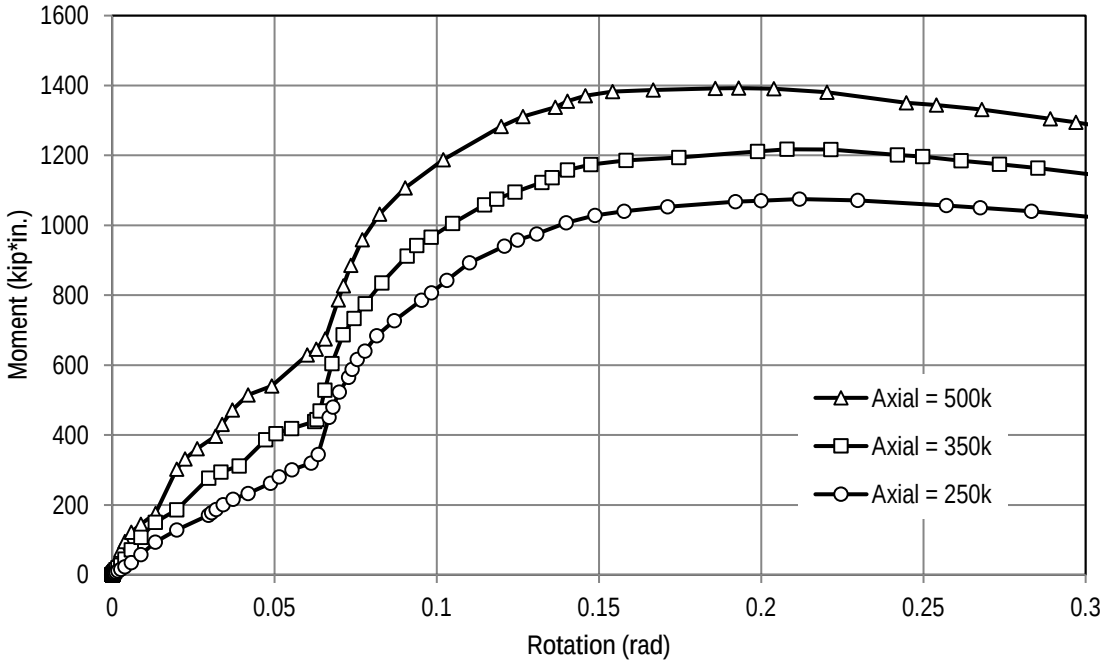

Figure 11: Effect of Axial Load for Centered Radiused Pin

There are a number of items of note between the results for the radiused pin in Figure 11 and the flat-bottom pin in Figure 10, chiefly:

- The initial stiffness of the flat-bottom pin is much greater than the radiused pin. This is evidenced by the steeper initial slope in Figure 10 versus Figure 11. This result is directly attributable to the fact that he radiused pin can rock (i.e. uplift) more easily on the base plate, thereby providing less internal restraint against overturning when compared to the flat-bottom pin.

- The maximum moment capacity is independent of the pin shape and occurs at approximately 0.17 radians for both the radiused and flat-bottom pin models. This occurs since the maximum moment coincides with a region where the cup dominates the contribution to the pin restraint, i.e., in a region that is largely independent of the shape of the base of the pin.

- The nonlinear region of both plots begins at approximately 0.07 radians. This is irrespective of the magnitude of the initial slope. In Figure 10, the initial stiffness is large followed by a plateau until 0.07 radians. This is consistent with the pin's initial self-restraint to overturning followed by tipping of the pin. In contrast, Figure 11 shows a relatively smaller initial stiffness without any plateau. This is consistent with a pin that starts rocking immediately upon load application. The net effect of the cup restraint is that the starting point occurs at roughly the same rotation, albeit at different magnitudes of moment.

4.3 Effects on Frame Modeling

The results from the previous two section including both the radiused and flat-bottom pin are input into OpenSees to assess the pin-cup support condition's effect on the frame stability. The results for the case of a centered, radiused and flat-bottom pin with axial load equal to 500 kips are plotted against the theoretical boundary conditions of pinned and fixed in Figure 12. The abscissa is the vertical displacement of the column at the top of the frame (in inches) and the ordinate is the force applied to the frame normalized to the load at which the fixed-base case becomes unstable.

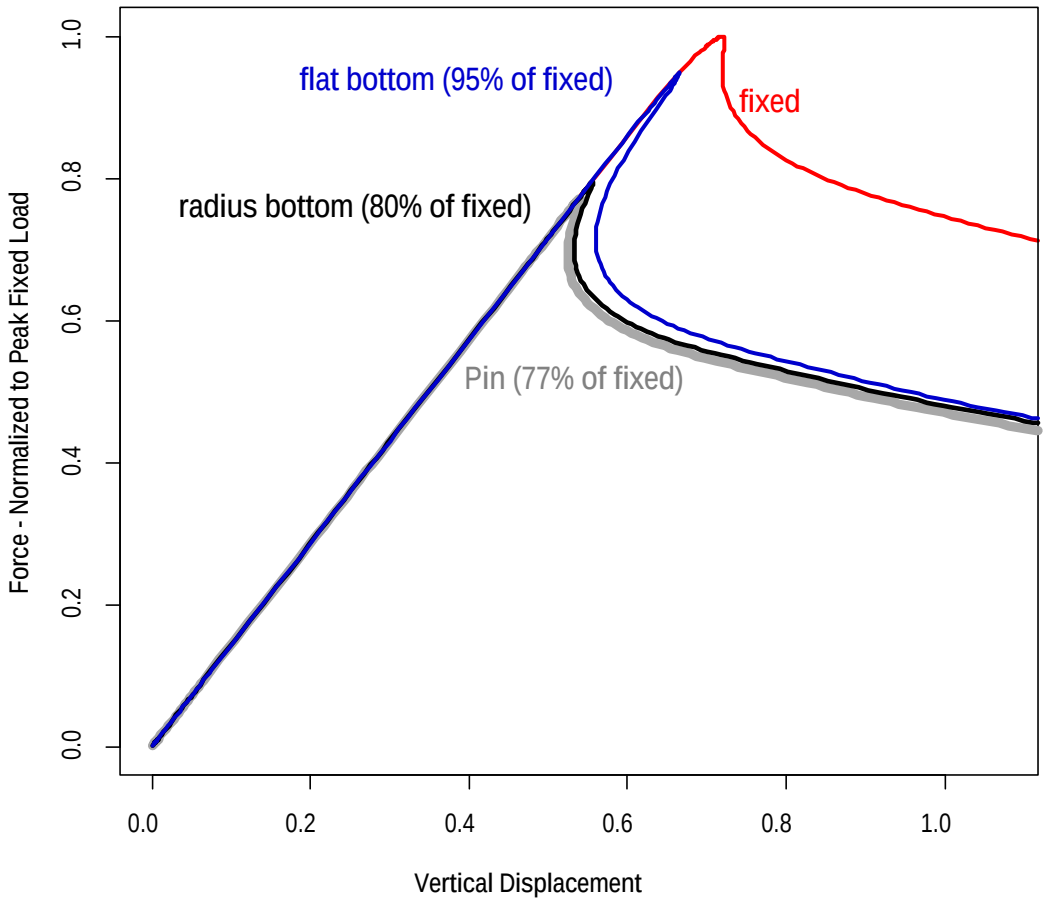

Figure 12: Load-deflection Results from OpenSees

As predicted by the initial OpenSees analyses and consistent with theory, the case with a fixed base shows the highest applied force and the case with a pinned base shows the lowest applied force at which the frame becomes unstable.

The case of the radiused pin produces a frame response that is very similar to the pinned condition (approximately 4% greater). This result might be intuitive, since the curvature of the pin limits the restraint provided by the pin to overturning. In the limit that the radius of the curve is decreased such the base of the pin approaches a knife edge, the solution would be expected to track even closer to the pinned condition. The slight increase in frame buckling capacity is likely attributable to the interaction between the pin and the cup.

The case of the flat-bottom pin provides a significant increase in the frame buckling capacity over that of the theoretical pin or radiused pin condition. A majority of the increase is attributable to the pin reacting on the base along its contact surface under large axial load. After the pin begins to tip toward the cup, the restraint to overturning decreases but contact with the cup begins to offer some restraint, however, the initial buckling has already begun. The effect of the cup restraint is expected to be limited, as evidenced by the results of the radiused pin case discussed in the previous paragraph. Furthermore, the magnitude of moment transferred to the base in the "flat" case is significant. The introduction of the radius significantly reduces the moment transfer to the base.

5. Conclusion

The analyses performed and subsequent discussion herein have shown that a marked effect may be captured by accurately modeling boundary conditions. For the specific geometry shown here, the radiused pin showed little improvement over the case of the pinned condition and may be considered not worth the extra computational effort required to perform refined finite element analysis (FEA) on the support components. The flat-bottom pin did, however, provide a significant increase in the buckling capacity of the frame (about 23%). Furthermore, the flat-bottom case provides a capacity similar to the fixed-end case, therefore potentially validating the use of a refined FEA to capture the complicated effect.

Ultimately, the decision on whether to model individual components or sub-assemblies with robust FEA rests with the engineer. This paper highlighted the pronounced effect of one such connection model (flat-bottom pin), but also showed the relative insignificance of another (radiused pin). Knowing which model will yield helpful results *a priori* is often difficult. Therefore, the authors recommend first bounding the solution with analyses based on simple boundary condition assumptions such as the pinned or fixed base conditions discussed in the paper, and then adding refinement where construction details suggest that the simplifying assumptions may be too rudimentary for the intended analysis.

Disclaimer

The views expressed herein are solely those of the authors and do not necessarily represent the position(s) of Exponent Inc., Risk Management Solutions, Inc., or any individuals therein.

References

Abaqus (2011). Version 6.11-1. Dassault Systemes.

AISC 303-10. *Code of Standard Practice for Steel Buildings and Bridges*. American Institute of Steel Construction. Chicago, IL. April 14, 2010.

AISC 360-10. *Specification for Structural Steel Buildings*. American Institute of Steel Construction. Chicago, IL. June 22, 2010.

Chen, W.F. and Lui, E.M. (1987). Structural Stability: Theory and Implementation. Prentice-Hall, Inc. Upper Saddle River, NJ.

Leet, Kenneth M. and Uang, Chia-Ming (2005). Fundamentals of Structural Analysis. Second Edition. McGraw Hill Higher Education. San Francisco, CA.

Steel Interchange (1992). *Modern Steel Construction*. Chicago, IL. April.

OpenSees (2013). "Open System for Earthquake Engineering Simulation". Pacific Earthquake Engineering Research Center. Version 2.4.4 (rev 5764). The Regents of the University of California. http://opensees.berkeley.edu

Souza, R.M (2000), *Force-based Finite Element for Large Displacement Inelastic Analysis of Frames*, Doctoral Dissertation, Department of Civil and Environmental Engineering, University of California, Berkeley, Fall 2000

Timoshenko, Stephen P. and Gere, James M. Theory of Elastic Stability. Second Edition. Dover Publications, Inc. Mineola, NY.